J|A|C|S
ARTICLES
Published on Web 12/28/2001

Theoretical Studies of Magnetic Interactions in Mn(II)(hfac)$_2${di(4-pyridyl)phenylcarbene} and Cu(II)(hfac)$_2${di(4-pyridyl)phenylcarbene}

Yu Takano,*,† Yasutaka Kitagawa,† Taku Onishi,† Yasunori Yoshioka,† Kizashi Yamaguchi,*,† Noboru Koga,*,‡ and Hiizu Iwamura§

Contribution from the Department of Chemistry, Graduate School of Science, Osaka University, Toyonaka, Osaka 560-0043, Japan, Department of Chemo-Pharmaceutical Sciences, Graduate School of Pharmaceutical Sciences, Kyushu University, Fukuoka 812-8582, Japan, and University of the Air, Chiba 261-8586, Japan

Received April 7, 2001. Revised Manuscript Received August 15, 2001

Abstract: Bis(hexafluoroacetylacetonato(hfac))manganese(II) coordinated with di(4-pyridyl)phenylcarbene, Mn(II)(hfac)$_2${di(4-pyridyl)phenylcarbene} (**1a**) and its copper analogue Cu(II)(hfac)$_2${di(4-pyridyl)phenylcarbene} (**2a**) have attracted great interest from the viewpoint of photoinduced magnetism. The complexes **1a** and **2a** are regarded as the new d−π−p conjugated systems containing transition metal ion and carbene as spin sources. The magnetic measurements demonstrated antiferromagnetic and ferromagnetic effective exchange interactions for **1a** and **2a**, respectively. Here, we have performed UHF and UHF plus DFT hybrid calculations (UB3LYP) to elucidate the nature of the through-bond effective exchange interaction between Mn(II) (or Cu(II)) ion and triplet carbene sites in **1a** (or **2a**) and their model complexes. The natural orbital analysis of the UHF and UB3LYP solutions and CASCI calculations for the simplest models of **1a** and **2a** are performed to elucidate relative contributions of spin polarization (SP) and spin delocalization (SD) (or superexchange (SE)) interactions for determination of the sign of J_{ab} values. Mn(II) carbene complex **1a** shows an antiferromagnetic interaction because of the π-type antiferromagnetic SE effect and the π-type SP effect, while the positive J_{ab} value for Cu(II) carbene complex **2a** can be explained by the fact that ferromagnetic SE and SP interactions due to orbital orthogonality are more effective than the σ-type antiferromagnetic SE interaction. The ligand coordination effects of both 4-pyridylcarbene and hfac play crucial roles for determination of the J_{ab} values, but the ligand coordination effect of hfac is more important for the active control of charge or spin density distributions than that of 4-pyridylcarbene. The spin alignment mechanisms of **1a** and **2a** are indeed consistent with SE plus SP rule, which is confirmed with the shape and symmetry of natural orbitals, together with charge and spin density distributions.

Introduction

Recently molecular magnetism has been one of the central issues in molecular science. The molecule-based magnetic compounds[1] have indeed attracted both experimental and theoretical attention in relation to possible candidates of ferro- or ferri-magnet, magnetic conductor,[2] spin-mediated superconductor,[3] and so on. Their magnetic properties may also be controlled or switched by several procedures such as photoexcitation.[4] Molecule-based magnets are not only important for elucidation of spin alignment mechanisms but also promising as building blocks of magnetic materials from the practical viewpoint of materials synthesis. Such bottom-up strategy becomes more and more significant for development of molecule-based electronic, magnetic, and optical devices.

The d−p conjugated system[1,5−7] constructed of organic free radicals and transition metal ions appears to be one of the most promising candidates for molecule-based magnetic materials.

* Corresponding authors. Y.T.: (phone) +81-6-6850-5405; (fax) +81-6-6850−5550; (e-mail) ytakano@chem.sci.osaka-u.ac.jp. K.Y.: (phone) +81-6-6850-5404; (fax) +81-6-6850-5550; (e-mail) yama@chem.sci.osaka-u.ac.jp. N.K.: (e-mail) koga@phar.kyushu-u.ac.jp.

† Osaka University.

‡ Kyushu University.

§ University of the Air.

(1) (a) Gatteschi, D.; Kahn, O.; Miller, J. S.; Palacio, F. Eds. *Magnetic Molecular Materials*; Kluwer Academic Publishers: Dordrecht, 1991. (b) Miller, J. S.; Epstein, A. J. Angew. *Chem., Int. Ed. Engl.* **1994**, *33*, 385. (c) Kahn, O., Ed. *Magnetism: A Supramolecular Function*; NATO ASI Series C, Vol. 484,; Kluwer Academic Publishers: Dordrecht, 1996. (d) Conorado, E., Delhais, P., Gatteschi, D., Miller, J. S., Eds. *Molecular Magnetism: From Molecular Assemblies to the Devices*; NATO ASI Series E, Vol. 321; Kluwer Academic Publishers: Dordrecht, 1996. (e) Itoh, K.; Kinoshita, M. Eds. *Molecular Magnetism*: *New Magnetic Materials*; Kodansha-Godon and Breach: Tokyo, 2000.

(2) (a) Mitani, M.; Takano, Y.; Yoshioka Y.; Yamaguchi, K. *J. Chem. Phys.* **1999**, *111*, 1309. (b) Mitani, M.; Mori, H.; Takano, Y.; Yamaki, D.; Yoshioka Y.; Yamaguchi, K. *J. Chem. Phys.* **2000**, *113*, 4035. (c) Mitani, M.; Yamaki, D.; Yoshioka, Y.; Yamaguchi, K. *J. Chem. Phys.* **1999**, *111*, 2283.

(3) (a) Yamaguchi, K. *Int. J. Quantum Chem.* **1990**, *31*, 167. (b) Nagao, H.; Mitani, M.; Nishino, M.; Yoshioka, Y.; Yamaguchi, K. *Int. J. Quantum Chem.* **1997**, *65*, 947. (c) Yamaguchi, K.; Kitagawa, Y.; Onishi, T.; Isobe, H.; Kawakami, T.; Nagao, H. *Coord. Chem. Rev.*, in press.

(4) (a) Gatteschi, D.; Yamaguchi, K. In *Molecular Magnetism: From Molecular Assemblies to the Devices*; Conorado, E., Delhais, P., Gatteschi, D., Miller, J. S., Eds.; NATO ASI Series E, Vol. 321; Kluwer Academic Publishers: Dordrecht, 1996; p 561. (b) Nishino, M.; Yamaguchi, K.; Miyashita, S. *Phys. Rev.* **1998**, *B58*, 9303. (c) Nagao, H.; Nishino, M.; Shigeta, Y.; Yoshioka, Y.; Yamaguchi, K. *J. Chem. Phys.* **2000**, *113*, 11237.

(5) Stumpf, H. O.; Ouahab, L.; Pei, Y.; Grandjean, D.; Kahn, O. *Science* **l993**, *261*, 447.

10.1021/ja015967x CCC: $22.00

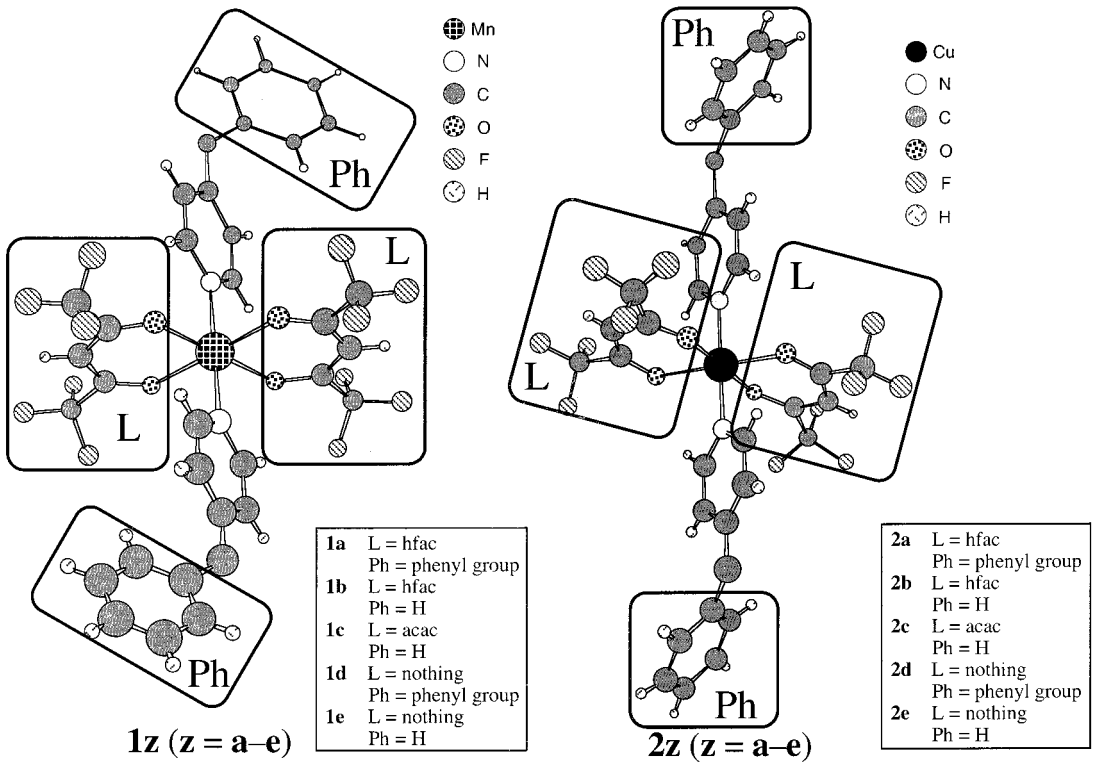

Figure 1. Molecular structures of Mn(II)(hfac)$_2${di(4-pyridyl)phenylcarbene} (**1a**), Cu(II)(hfac)$_2${di(4-pyridyl)phenylcarbene}(**2a**), and the model complexes **1b**−**1e** and **2b**−**2e** for **1a** and **2a**, respectively.

In these d−p conjugated spin systems, organic radicals serve as spin carriers as well as ligands to magnetic metal ions.[1] Therefore, we can design various types of magnetic molecules with parallel and antiparallel spin configurations by suitable combinations of building blocks, since magnetic molecules are constructed with two parts of a spin source and a coupling unit such as a π conjugated system. Experimental efforts[1,5−7] to synthesize magnetic dendrimers[8] and polymers[6,9] have been made extensively, and magnetic couplings in these species have been determined by magnetic measurement techniques.[1]

Iwamura, Koga, and their collaborators prepared bis(hexafluoroacetylacetonato(hfac))manganese(II) coordinated with di(4-pyridyl)phenylcarbene, Mn(II)(hfac)$_2${di(4-pyridyl)phenylcarbene} (**1a**) and its copper analogue, Cu(II)(hfac)$_2${di(4-pyridyl)phenylcarbene} (**2a**) (see Figure 1), by photolysis of the precursor transition metal complexes.[10−12] Magnetic measurements on the precursor complex of Mn(hfac)$_2$ or Cu(hfac)$_2$ with diazodi(4-pyridyl)phenylmethane indicated that the effective exchange interaction (J_{ab}) between the transition metal ions M(II) (M = Mn, Cu) through the diazodi(4-pyridyl)phenylmethane group is essentially zero, namely, J_{ab}(M(II)−M(II)) ≅ 0. On the other hand, after irradiation to generate the triplet carbene site, the J_{ab} value between Mn(II) and carbene via the 4-pyridyl group was found to be about −12.37 cm^{-1},[10] while the J_{ab} value for the Cu(II)−carbene pair was demonstrated to be ferromagnetic.[11] Iwamura, Koga, and their collaborators further reported that a 1:1 complex of Mn(II)(hfac)$_2$ with (4-pyridyl)phenylcarbene formed helical and zigzag infinite chains with trans and cis coordinations of pyridyl nitrogen atoms to Mn(II), respectively. The antiferromagnetic exchange coupling parameters (J_{ab}) for the former (**3T**) and latter (**3C**) chains were −16.96 and −24.18 cm^{-1}, respectively. On the other hand, the copper analogue (**4T**) with the trans coordination structure exhibited the large positive J_{ab} value (46.43 cm^{-1}).[11] Despite development of the experiments on d−π−p conjugated spin systems,[1,10−12] theoretical work with them at the ab initio level is still insufficient.

Magnetism is a characteristic property in strongly electron correlated systems. The d−π−p conjugated complexes under present consideration are regarded as such electron-correlated systems. It is desiable to perform post Hartree−Fock (HF) calculations such as coupled-cluster (CCSD(T)) and CASPT2 in order to investigate the magnetic interaction of d−π−p conjugated complexes as in the case of π−π conjugated organic polyradicals.[2] However, they are impossible for these large systems. In recent years, density functional (DFT) calculations[13−16]

(6) (a) Iwamura, H.; Inoue, K.; Hayamizu, T. *Pure Appl. Chem.* **l996**, *68*, 243. (b) Kitano, M.; Ishimaru, Y.; Inoue, K.; Koga, N.; Iwamura, H. *Inorg. Chem.* **l994**, *33*, 6012. (c) Ishimaru, Y.; Kitano, M.; Kumada, H.; Koga, N.; Iwamura, H. *Inorg. Chem.* **l998**, *37*, 2273.
(7) Caneshi, A.; Gatteschi, D.; Sessoli, R.; Rey, P. *Acc. Chem. Res.* **1989**, *22*, 392.
(8) (a) Rajca, A.; Rajca, S. *J. Am. Chem. Soc*., **1996**, *118*, 8121. (b) Rajca, A.; Lu, K.; Rajca, S. *J. Am. Chem. Soc.* **1997**, *119*, 10335. (c) Rajca, A.; Wongsriratankul, J.; Rajca, S.; Cerny, R., *Angew. Chem., Int. Ed. Engl.* **1998**, *37*, 1229. (d) Kumada, H.; Sakane, A.; Koga N.; Iwamura, H. *J. Chem. Soc., Dalton Trans.* **2000**, 911.
(9) (a) Yoshioka, N.; Pahti, P. M.; Kaneko, T.; Kuzumaki, Y.; Tsuchida, E.; Nishide, H., *J. Org. Chem.* **1994**, *59*, 4272. (b) Nishide, H.; Kaneko, T.; Nii, T.; Katoh, K.; Tsuchida, E.; Yamaguchi, K. *J. Am. Chem. Soc*., **1995**, *117*, 548. (c) Kamachi, M.; Kajiwara, A.; Mori, W.; Yamaguchi, K. *Mol. Cryst. Liq. Cryst.* **1995**, *273*, 117.
(10) Koga, N.; Ishimaru, Y.; Iwamura, H. *Angew. Chem., Int. Ed. Engl.* **1996**, *35*, 175.
(11) Sano, Y.; Tanaka, M.; Koga, N.; Matsuda, K.; Iwamura, H.; Rabu, P.; Drillon, M. *J. Am. Chem. Soc.* **1997**, *119*, 8246.
(12) Karasawa, S.; Sano, Y.; Akita, T.; Koga, N.; Itoh, T.; Iwamura, H.; Rabu, R.;. Drillon, M. *J. Am. Chem. Soc.* **l998**, *129*, 10080.
(13) Parr R. G.; Young, W. *Density Functional Theory of Atoms and Molecules*; Oxford University Press: Oxford, 1989.
(14) Trickey, S. B., Ed. *Density Functional Theory of Many-Fermion Systems*; Advances in Quantum Chemistry 21; Academic Press: San Diego, 1990.

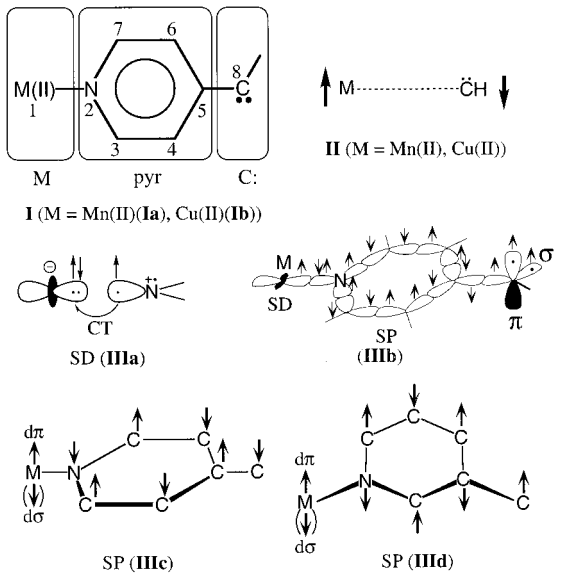

Figure 2. Through-bond interaction model of M(II)(4-pyridyl)carbene (**I**), direct effective exchange interaction (**II**) between transition metal ion (M) and CH, spin delocalization (SD) mechanism (**IIIa**) between dσ electron of transition metal ion (M) and lone pair electrons of nitrogen atom in 4-pyridyl ring, the σ-type spin polarization (SP) mechanism (**IIIb**) through the 4-pyridyl ring for σ and π electrons of triplet carbene, and the π-type SP interactions (**IIIc** and **IIId**) of 4- and 3-pyridylcarbenes with dσ or dπ electron of M(II).

have been performed on large molecules to elucidate various properties such as binding and excitation energies. DFT has been accepted as an alternative approach for the post HF methods. In another series of papers,[2,17] we thoroughly examined the applicability of DFT to organic polyradicals and magnetic polymers. We concluded that DFT employing appropriate exchange-correlation functionals is practically useful for elucidation of electronic and magnetic properties of these species.

Previously,[18,19] we performed unrestricted Hartree−Fock (UHF), UHF Møller−Plesset *n*th(n = 2,4)-order perturbation (UMPn), UHF coupled cluster (UCCSD(T)), DFT (UBLYP), and HF plus DFT hybrid (UB3LYP) calculations using several basis sets for the simplest model complexes, (e.g., M(4-pyridyl)-carbenes (M = Mn(II) and Cu(II)) (**Ia** and **Ib**) as shown in Figure 2) to elucidate the magnitude of the J_{ab} values between the transition metal and carbene sites. The UCCSD(T) results for these models were consistent with the experiments by Iwamura et al.,[10−12] while the magnitude of the J_{ab} values was too large under the DFT approximation. This indicated that the coordination ligands such as hfac could not be neglected for precise calculations of the J_{ab} values in these complexes. However, post HF calculations such as UCCSD(T) for them are time-consuming.

Recently,[20] Musin and Morokuma investigated the electronic structure, spin density distribution, and mechanisms of exchange interactions in the series of complexes of Cu(II)(hfac)$_2$, Mn(II)(hfac)$_2$, and Cr(III)(mesotetraphenylporphyrinato) with 3- and 4-(*N*-oxyl-*tert*-butylamino)pyridines (3NOPy and 4NOpy). They showed that the contribution of indirect one-center exchange interaction to total exchange interaction in the complexes is predominant and allows one to give a possible explanation of the magnetic properties of such types of complexes.

In this joint study between theory[18,19] and experiments,[10−12] we performed UHF and HF plus DFT hybrid calculations (HDFT) such as UB3LYP to elucidate the nature of magnetic interactions in Mn(II)(hfac)$_2${di(4-pyridyl)phenylcarbene} (**1a**)[10] and Cu(II)(hfac)$_2${di(4-pyridyl)phenylcarbene} (**2a**).[11] Several model complexes (**1b**−**1e** and **Ia** for **1a** and **2b**−**2e** and **Ib** for **2a**) shown in Figure 1 have been also examined to clarify the ligand coordination effects in the complexes. The natural orbital analysis of the UHF and HDFT solutions of **1z** and **2z** (**z** = **a**−**e**) and CASCI calculations for **Ia** and **Ib** are performed to elucidate relative contributions of spin polarization (SP) and spin delocalization (SD) (or superexchange (SE)) interactions for determination of the sign of J_{ab} values. Implications of the calculated results have been discussed in relation to the photoinduced molecular magnetism of **1z** and **2z** (**z** = **a**−**e**)[10,11] from the viewpoint of charge and spin density distributions, as well as the shape and symmetry of natural orbitals. Finally, spin alignment rules for d−π−p conjugated polyradicals via SD, SP, and other mechanisms are discussed using the calculated results in combination with the experimental results available.[10−12]

Theoretical Background

Computation of Effective Exchange Integrals. The effective exchange interactions (J_{ab}) between magnetic sites in the highest- (HS) or the lowest- (LS) spin complexes have been described by the Heisenberg (HB) model, from experimental grounds[1,21,22]

$$H(\mathrm{HB}) = -2\sum J_{ab}\mathbf{S_a}\cdot\mathbf{S_b} \qquad (1)$$

where $\mathbf{S_a}$ and $\mathbf{S_b}$ represent the spins at sites a and b, respectively. J_{ab} can be experimentally determined by the measurement of magnetic susceptibility.[1] Recent developments of ab initio computational techniques such as UHF and UCCSD(T), together with the spin-polarized DFT (UDFT) methods, have enabled us to calculate J_{ab} values for the present d−π−p conjugated systems,[18,19] leading to the design of molecule-based magnets. In fact, the UHF and UDFT solutions for the LS states of magnetic transition metal complexes usually exhibit a broken-symmetry (BS) problem.[18,19,23−31] Therefore, spin projection of

(15) Labanowski, J. K., Andzelm, J. W. Eds. *Density Functional Methods in Chemistry*; Springer-Verlag: New York, 1991.
(16) (a) Seminario, J. M., Politzer, P., Eds. *Theoretical and Computational Chemistry, Vol. 2, Modern Density Functional Theory: A Tool for Chemistry*; Elsevier: Amsterdam, 1995. (b) Seminario, J. M., Ed. *Theoretical and Computational Chemistry, Vol. 4, Recent Developments and Applications of Modern Density Functional Theory*; Elsevier: Amsterdam, 1996.
(17) (a) Kawakami, T.; Yamanaka, S.; Takano, Y.; Yoshioka, Y.; Yamaguchi, K. *Bull. Chem. Soc. Jpn.* **1998**, *71*, 2097. (b) Mitani, M.; Yamaki, D.; Takano, Y.; Kitagawa, Y.; Yoshioka, Y.; Yamaguchi, K. *J. Chem. Phys.* **2000**, *113*, 10486. (c) Soda, T.; Kitagawa, Y.; Onishi, T.; Takano, Y.; Shigeta, Y.; Nagao, H.; Yoshioka, Y.; Yamaguchi, K. *Chem. Phys. Lett.* **2000**, *319*, 223.
(18) Takano, Y.; Soda, T.; Kitagawa, Y.; Yoshioka, Y.; Yamaguchi, K. *Chem. Phys. Lett.* **1999**, *301*, 309.
(19) Takano, Y.; Soda, T.; Kitagawa, Y.; Onishi, T.; Yoshioka, Y.; Yamaguchi, K. *Int. J. Quantum Chem.* **2000**, *80*, 681.
(20) Musin, R. N.; Morokuma, K. *Abstract of Papers of the 7th International Conference on Molecule-Based Magnets*, San Antonio, TX, September 16−21, 2000.
(21) Kawakami, T.; Yamanaka, S.; Yamada, S.; Mori, W.; Yamaguchi, K. In *Molecule-Based Magnetic Materials, Theory, Technique and Applications*; Turnbull, M. M., Sugimoto, T., Thompson, L. K., Eds.; ACS Symposium Series 644; American Chemical Society: Washington, DC, 1996; p 30.
(22) Salem, L. *Electrons in Chemical Reactions: First Principle*; John Wiley and Sons: New York, 1982; Chapter 7.
(23) Yamaguchi, K.; *Chem. Phys. Lett.* **1975**, *33*, 330. (b) Yamaguchi, K. *Chem. Phys. Lett.* **1979**, *66*, 395.
(24) Anderson, P. W. *Solid State Phys.* **1963**, *14*, 99.
(25) Ginsberg, A. P. *J. Am. Chem. Soc.* **1980**, *102*, 111.

the BS solutions should be carried out to eliminate spin contamination in spin-polarized DFT and UHF methods. A useful scheme for spin projection has been developed on the basis of the isotropic HB Hamiltonian combined with UHF and UDFT calculations.[17−19,27] The spin projections of these solutions are performed by assuming energy splitting of the HB model, providing a practical computational scheme for J_{ab} values for linear uniform chains with N spin sites.[2,17] Our spin projection scheme has been applied to triplet methylene clusters $(CH_2)_N$ ($N = 2-11$)[17] and polycarbenes with a *m*-phenylene bridge ($N = 2-10$),[2] providing reasonable J_{ab} values as compared to the experiments. The computational scheme is size-consistent,[17] leading to a simple equation for the present case ($N < 4$) as

$$J_{ab}(\mathrm{AP-X}) = \frac{^{LS}E_X - {}^{HS}E_X}{^{HS}\langle S^2\rangle_X - {}^{LS}\langle S^2\rangle_X} \quad (X = \mathrm{UHF, DFT};\ N = 2 \text{ or } 3) \quad (2)$$

where ${}^{Y}E_X$ and ${}^{Y}\langle S^2\rangle_X$ denote the total energy and total spin angular momentum of the spin state Y by the calculated method X, respectively. The J_{ab} values were also calculated by the spin-unprojected scheme on the basis of an assumption of the negligible orbital overlap between magnetic orbitals[17]

$$J_{ab}(X) = \frac{^{LS}E_X - {}^{HS}E_X}{4(N-1)S_aS_b} \quad (X = \mathrm{UHF, DFT};\ N > 1) \quad (3)$$

where $S_a = {}^5/_2$ and ${}^1/_2$ for the Mn(II) and Cu(II) ions, respectively, and $S_b = {}^2/_2$ for the triplet carbene. N is the site number ($N = 3$ for **1z** and **2z**). The difference between J_{ab}(AP-X) and J_{ab}(X) is responsible for the orbital overlap effects.[17] However, it is noteworthy that the signs of J_{ab}(X) and J_{ab}(AP-X) are the same as can be recognized from eqs 2 and 3.

The above BS results for d−π−p conjugated systems should be examined using the symmetry-adapted multiconfiguration methods for quantitative purpose. Configuration interaction (CI)-type methods such as the complete active space (CAS) CI are applicable in order to elucidate not only the reliability of the BS DFT approaches but also the spin alignment mechanisms. J_{ab} values can be calculated using the energy gap between symmetry-adapted LS and HS states as follows:

$$J_{ab}(\mathrm{CASCI}) = \frac{^{LS}E_{CASCI} - {}^{HS}E_{CASCI}}{S_{HS}(S_{HS}+1) - S_{LS}(S_{LS}+1)} \quad (4)$$

where ${}^{Y}E_{CASCI}$ denotes the total energy of the spin state Y by the CASCI method[2]; $S_{HS} = {}^7/_2$ and ${}^3/_2$ and $S_{LS} = {}^3/_2$ and ${}^1/_2$ for **Ia** and **Ib**, respectively. Equation 2 is reduced to eq 4 if the spin contamination in UHF and UDFT is small. The CASCI can be used to elucidate the SOMO−SOMO and SP plus other contributions to effective exchange integrals.[18,19]

Spin Alignment Rules Based on the Configuration Interaction Model. Let us consider the orbital symmetry rule[18,19,32] for the d−π−p conjugated systems. Here, we utilize the intermolecular CI[21] picture for **1z** and **2z** (**z** = **a**−**e**) in order to investigate the mechanism of the effective exchange interactions for **1a** and **2a**. **1z** and **2z** have three magnetic sites. However, reported experimental results[10,11] showed that the J_{ab} values between the nearest neighbors play important roles to determine their magnetic properties. The two-radical-site model (**I**) in Figure 2 can be used for theoretical consideration of the effective exchange interactions. The model is formally divided into M(II) (M = Mn and Cu), 4-pyridyl group (pyr), and carbene (C:) fragments as shown in **I** of Figure 2. The direct exchange interaction between M(II) and :CH in **II** should be essentially zero[33,34] because of relatively long intersite distance (R(Mn−CH) > 5.0 Å), as shown in Figure 2. Since the nitrogen site of 4-pyridyl group coordinates to the M(II) ion, the SD[21] mechanism should be operative between the d_{z^2} (dσ) half-occupied orbital of M(II) and N-lone pair as illustrated in **IIIa** of Figure 2. The through σ-bond interaction of the d_{z^2} (dσ) spin via the SP of the σ-bond network of 4-pyridyl group provides net ferromagnetic exchange integrals with π- and σ-radical electrons of the carbene group as shown in **IIIb**.[21] The SP mechanism[21] through the dπ(M)−π(4-pyridyl)−pπ(carbene) or dσ(M)−π-(4-pyridyl)−pπ(carbene) network should provide an antiferromagnetic or a ferromagnetic exchange interaction, respectively, as illustrated in **IIIc** of Figure 2, where we utilize the spin vector model for pictorial understanding of the SP effect.[17,21] The induced π-spin on the N-atom of the 4-pyridyl group via the SP mechanism interacts with the dσ or dπ orbital spin of M(II) in a ferro- and antiferromagnetic manner, respectively. The spin alignment rule via the SP mechanism is therefore reversed for the 3-pyridyl group as illustrated in **IIId**.

Next, we consider the charge-transfer (CT) interaction of M(II) with the π orbitals of the 4-pyridyl group as shown in Figure 3. The effective exchange interactions within CT configurations are antiferromagnetic due to the nonzero overlap integrals of the dπ(Mn(II))−π(second HOMO) or dπ(Mn(II))−π*(LUMO) orbitals, as illustrated in **IVa** and **IVb** of Figure 3. Their contributions are incorporated by the fourth-order perturbation (PT4) method,[21] and these are the origins of the antiferromagnetic SE interactions in the orbital symmetry rule. The ferromagnetic SE interactions are also conceivable because of the orthogonal orbital interactions of π-second HOMO (or π*-LUMO) with other d orbitals of M(II) such as the dσ orbital as shown in **IVc** and **IVd** of Figure 3.

Probably the total sum of the SE interactions in the Mn(II) complex (**1z**) remains antiferromagnetic because of the strong dπ−π(π*) orbital overlap integral. On the other hand, the SE interaction should be ferromagnetic in the Cu(II) complex (**2z**) because of the orthogonal dσ and π(π*) orbital interaction in **IVc** and **IVd**. Therefore, the J_{ab} value for **2z** should be positive because of ferromagnetic SE interaction, in addition to the ferromagnetic SP effect. Thus, the orbital symmetry rules are

(26) (a) Noodleman, L. *J. Chem. Phys.* **1981**, *74*, 5737. (b) Noodleman, L.; Davidson, E. R. *Chem. Phys.* **1986**, *109*, 131. (c) Noodleman, L.; Case, A. D. *Adv. Inorg. Chem.* **1992**, *38*, 423.
(27) (a) Yamaguchi, K.; Takahara, Y.; Fueno, *T.* In *Applied Quantum Chemistry*; Smith, V. H., Jr., Schaefer, H. F., III, Morokuma, K., Eds.; Reidel: Boston, 1986; p 155. (b) Yamaguchi, K.; Tsunekawa, T.; Toyoda, Y.; Fueno, T. *Chem. Phys. Lett.* **1988**, *143*, 371. (c) Yamaguchi, K.; Fueno, T.; Ueyama, N.; Nakamura, A.; Ozaki, M. *Chem. Phys. Lett.* **1989**, *164*, 210.
(28) Hait, J. R.; Rappe, A. K.; Gorun, S. M. Upton, T. H. *J. Phys. Chem.* **1992**, *96*, 6264.
(29) Alemany, E. P.; Alvarez, S.; Cano, J. *J. Am. Chem. Soc.* **1997**, *119*, 1297.
(30) Bencini, A.; Totti, F.; Daul, C. A.; Doclo, K.; Fantucci, P.; Barone, V. *Inorg. Chem.* **1997**, *36*, 5022.
(31) Ruiz, E.; Cano, J.; Alvarez, S.; Alemany, P. *J. Comput. Chem.* **1999**, *20*, 1391.
(32) Yamaguchi, K.; Yoshioka, Y.; Fueno, T. *Chem. Phys.* **l977**, *20*, 171.
(33) Yamanaka, S.; Kawamura, T.; Noro T.; Yamaguchi, K. *J. Mol. Struct. (THEOCHEM)* **1994**, *310*, 185.
(34) Sosa, R. M.; Gardiol, P.; Beltrame, G. *Int. J. Quantum Chem.* **l998**, *69*, 371.

Table 1. Spin Alignment Rules and Experimental Results for Several d−π−p Conjugated Systems

metal	type	SD (SE)	SP	total	experimental results[a,b]
Mn(II)(hfac)$_2$	para	$J_{SD} < 0$	$J_{SP} < 0$	$J_{total} < 0$	**1A** (−12.4), **3T** (−17.0), **9A** (<0), **lB** (−8.62), **3C** (−24.2), **9B** (−17)
Cu(II)(hfac)$_2$	para	$J_{SD} > 0$	$J_{SP} > 0$	$J_{total} > 0$	**2A** (>0), **2B** (40.7), **4T** (46.4), **6B** (2.96), **10A** (>0), **10B** (47)
	meta	$J_{SD} > 0$	$J_{SP} < 0$	$J_{total} > 0$ or < 0	**8B** (<0)
Cr(III)(TPP)	para	$J_{SD} < 0$	$J_{SP} < 0$	$J_{total} < 0$	**11B** (−53.6)
	meta	$J_{SD} < 0$	$J_{SP} > 0$	$J_{total} > 0$ or < 0	**12B** (8.5)

[a] The observed J_{ab} values (cm^{-1}) are given in parentheses. [b] The molecular structures for **1Z**−**12Z** are given in Figure 7.

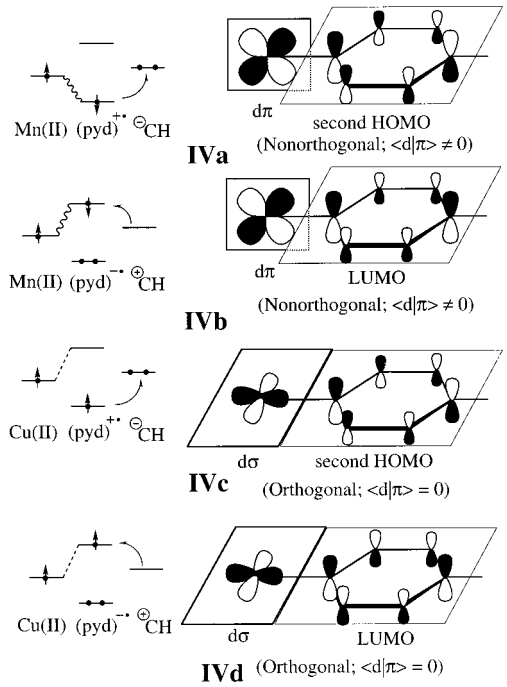

Figure 3. Antiferromagnetic superexchange interactions, **IVa** (dπ−π type), and **IVb** (dπ−π* type) between metal and 4-pyridyl moiety, respectively. **IVc** and **IVd** show the ferromagnetic SE interactions by orbital orthogonality. **IVc** is induced by the charge transfer from the pyridyl moiety to the carbene site, while **IVd** is induced by CT from the methylene site to the pyridyl moiety.

useful for qualitative explanation of the experimental tendency. The selection rule via the SE mechanism for the 4-pyridyl group is equally applicable to the Mn(II) or Cu(II) complexes with the 3-pyridyl group, since similar orbital overlap effects in Figure 3 are operative. Table 1 summarizes the SP plus SD (SE) spin alignment rules,[17,21,27] together with the experimental results available. From Table 1, the sign of the J_{ab} values in the meta-substituted systems is determined by subtle balances of the SP and SE effects. Moreover, quantitative calculations of the J_{ab} values are difficult on the basis of the CT models because of the nonorthogonality problem of the magnetic fragment orbitals.[21]

Natural Orbitals. Molecular orbital (MO) pictures would be desirable for deeper understanding of the magnetic interaction between M(II) and carbene via the 4-pyridyl ring, together with coordination ligands. A reliable procedure for this purpose is to perform the CASSCF calculations, which include all the configurations in aforementioned CI scheme, and the resulting natural orbitals (NOs) are utilized for MO theoretical explanation of magnetic interaction. But they are impossible for **1a** and **2a** because of too many π orbitals. Fortunately, the natural orbital analysis of UHF and UDFT solutions is a practical alternative to CASSCF as demonstrated previously.[2,17,21] Here, to obtain a MO theoretical explanation of the effective exchange interaction, the NOs of the UHF and UB3LYP solutions were determined by diagonalizing their first-order density matrices[2,17−19] as

$$\rho(\mathbf{r},\mathbf{r}') = \sum n_i\{\phi_i(\mathbf{r})\}^*\phi_i(\mathbf{r}') \qquad (5)$$

where n_i denotes the occupation number of NO ϕ_i. The occupation numbers of bonding and antibonding NOs were almost 2.0 and 0.0, respectively, except for the nine magnetic NOs for **1z**, and the five magnetic NOs for **2z**, for which the occupation numbers were close to 1.0. The bonding magnetic orbitals are generally given by the in- and out-of-phase combinations of the bonding (ϕ) and antibonding (ϕ^*) UHF NO (UNO) and DFT NO (DNO)

$$\psi_i{}^{\pm} = \cos\theta\phi_i \pm \sin\theta\phi_i^* \qquad (6)$$

where θ is the orbital mixing coefficient; $\theta \cong 45°$ for many magnetic orbitals.[17−19]

The orbital overlap $T_i = \langle\psi_i{}^+|\psi_i{}^-\rangle$ between magnetic orbitals is a measure of the SD (SE) effect; namely, $T_i = 0$ for pure metal biradical and $T_i = 1$ for the closed-shell pair.[17−19] The occupation numbers of the bonding and antibonding UNO-(DNO) are expressed by the T_i value; $n_i = 1 + T_i$, $n_i^* = 1 - T_i$. They are utilized for elucidation of SP effects of ligands and π-networks.

Computational Method

Geometries of the Complexes. In this study, we performed UHF and UB3LYP calculations for **1a**,[10] **2a**,[11] and these models (**1b**−**1e** and **2b**−**2e**) as shown in Figure 1 by using the Wachters'[35] (62111111/3312/32) plus Hay's diffuse basis sets[36] ($\alpha = 0.1054$ for Mn(II) and $\alpha = 0.1491$ for Cu(II)) for M(II), 6-31G* basis sets for C, N, O, and F, and 6-31G basis sets for H by Pople et al.[37,38] Then, we determined the NOs and their occupation numbers using eq 5. Other HDFT (spin-polarized Becke half and half LYP (UB2LYP)) and DFT (UBLYP) calculations were also carried out for **1z** and **2z** with the above basis sets. We summarized the results of UB2LYP and UBLYP calculation in the Supporting Information (Table S1−Table S10). Previously,[18,19] we examined the basis set dependence of the J_{ab} values. The present basis sets are useful enough for qualitative examination of them. However, we carried out previous calculations for **Ib** using smaller basis sets than Wachters' plus Hay's diffuse function. Therefore, we have utilized Wachters' plus Hay's diffuse function to calculate J_{ab} values for **Ib** in this work. In addition, we have evaluated the J_{ab} values for **Ia** and **Ib** by UNO CASCI methods, and these results have been utilized for confirmation of the BS calculations and estimation of the contribution between SP and SD effects.

The geometries of **1a** and **2a** (L = hfac; Ph = phenyl group) were taken from the X-ray crystallographic results[10,11] as shown in Figure 1. Their full geometry optimizations are impossible in our computer

(35) Wachters, A. J. H. *J. Chem. Phys.* **1970**, *52*, 1033.
(36) Hay, P. J. *J. Chem. Phys.* **1977**, *66*, 4377.
(37) Hariharan, P. C.; Pople, J. A. *Theor. Chim. Acta* **1973**, *28*, 213.
(38) Ditchfield, R.; Hehre, W. J.; Pople, J. A. *J. Chem. Phys.* **1971**, *54*, 724.

Table 2. Effective Exchange Integrals (J_{ab}(AP-X))[a] Calculated for Mn(II)(hfac)$_2${di(4-pyridyl)phenylcarbene} (**Iz**) and Cu(II)(hfac)$_2$ {di(4-pyridyl)phenylcarbene}(**2z**) (**z** = **a**−**e**) by UHF and UB3LYP Methods[b,c]

	Iz[d]					**2z**[e]			
methods X	**Ia**	**Ib**	**Ic**	**Id**	**Ie**	**2a**	**2b**	**2c**	**2e**
UHF	−2.722	−2.640	−1.922	−27.86	−28.81	134.9	135.8	135.6	35.90
	(−2.723)	(−2.640)	(−1.923)	(−27.78)	(−28.73)	(136.0)	(136.9)	(136.7)	(35.98)
UB3LYP	−10.06	−8.576	−8.637	−187.7	−73.76	67.14	66.15	64.20	*f*
	(−10.07)	(−8.580)	(−8.641)	(−192.1)	(−74.32)	(67.29)	(66.33)	(64.36)	*f*

[a] J_{ab} from eq 2 are shown in cm^{-1}. [b] The geometries were taken from refs 10 and 11. [c] The J_{ab}(X) values from eq 3 are given in parentheses. [d] J_{ab} from the experiment is −12.37 cm^{-1}. [e] J_{ab} from the experiment is 46.43 cm^{-1}. [f] The calculations were not converged.

system. We constructed simplified models (**1b**−**1e** and **2b**−**2e**) of **1a** and **2a** as shown in Figure 1. **1b** and **2b** are obtained by substitution of terminal phenyl groups of **1a** and **2a** (L = hfac; Ph = H) with hydrogen atoms. The geometries of them were the same as **1a** and **2a** except for C−H = 1.08 Å at the carbene site. **1c** and **2c** are given by substitution of hfac in **1b** and **2b** with acetylacetone (acac) ligands (L = acac; Ph = H). **1d** and **2d** are constructed by removal of hfac in **1a** and **2a** (L = nothing; Ph = phenyl group). **1e** and **2e** are obtained by removal of hfac in **1c** and **2c** (L = nothing; Ph = H). The calculated results will clarify the roles of coordination ligands for the J_{ab} values. UHF, DFT, and hybrid DFT computations were carried out by using the Gaussian94 program package,[39] while UNO CASCI calculations were performed using the GAMESS program package.[40]

DFT Calculation. In the DFT calculations, exchange-correlation energies[13−16,41−44] are generally defined by

$$E_{XC} = C_1 E_X^{HF} + C_2 E_X^{Slater} + C_3 \Delta E_X^{Becke88} + C_4 E_C^{VWN} + C_5 \Delta E_C^{LYP} \quad (7)$$

where the first and second terms in the right-hand of eq 7 indicate HF and Slater exchange functionals, respectively. The third and fourth terms mean Becke's exchange correction[41] involving the gradient of the density and Vosko, Wilk, and Nusair (VWN) correlation functional,[42] respectively, and the last term is the correlation correction of Lee, Yang, and Parr (LYP),[43] which includes the gradient of the density. C_i (i = 1−5) are the mixing coefficients. For example, the parameter sets (C_1, C_2, C_3, C_4, C_5) are taken as (0.2, 0.8, 0.72, 1.00, 0.81) for B3LYP and (0.5, 0.5, 0.5, 1.0, 1.0) for Becke half and half LYP (B2LYP), respectively.[44]

Spin-Adapted Calculations. We can select active orbitals for magnetic interactions by using occupation numbers in eq 5. First, to investigate the reliability of the BS DFT methods and to estimate direct exchange interaction between SOMOs, the full CI calculations within the seven (three) magnetic orbitals and seven (three) electrons {7, 7} ({3, 3}) were carried out for LS and HS states of molecule **Ia** (**Ib**), and the J_{ab} values were calculated by eq 4. Next, the full CI calculations were also performed by expanding the number (m) of active UNOs and number (n) of active electrons {m, n}: {11, 11} for **Ia** includes the four π-UNOs of the pyridyl group in addition to the seven SOMOs and {9, 9} for **Ib** contains the six π-UNOs of the pyridyl group with SOMOs. The UNO CI {7, 7} and {3, 3} results are responsible for the SOMO−SOMO interactions of **Ia** and **Ib**, respectively. These full CI calculations within the CAS {11, 11} and {9, 9} are referred to as UNO CASCI, which incorporates the SP and electron correlation (EC) effect of paired orbitals by the exchange interactions with SOMO electrons and other high-order excitations. Here, UNO CASCI {m, m} were carried out for both the LS and HS states using the UNO obtained from the LS singlet state.[17−19,21]

Computational Results of Manganese and Copper Complexes 1 and 2

Calculated J_{ab} Values and Charge and Spin Densities. Table 2 summarizes J_{ab} values calculated for the full model (**1a, 2a**) and simplified models (**1b**−**1e**, **2b**−**2c, 2e**) of the manganese and copper complexes by AP methods (eq 2). No reasonable UB3LYP results for **2d** and **2e** have been obtained because of the strong charge transfer from 4-pyridylcarbene to Cu(II). The J_{ab} values calculated by the unprojected method (eq 3) are also given in Table 2.

All the calculated values for **1** are negative in accordance with the experiments,[10,11] showing an antiferromagnetic through-bond interaction between Mn(II) and carbene sites via the 4-pyridyl group. The UHF underestimates the magnitude of the J_{ab} value for **1** as compared with the experimental value (−12.37 cm^{-1}).[10] The J_{ab} values by UB3LYP reproduce the experimental value[10] quantitatively. On the other hand, all the J_{ab} values for **2** show ferromagnetic couplings between Cu(II) and carbene sites via the 4-pyridyl group. The J_{ab} values by UB3LYP reproduce the experimental value (46.43 cm^{-1}).[11] UHF overestimates the ferromagnetic interaction. Judging from the previous result,[18,19] UCCSD(T) will be necessary for reliable post HF calculations of the J_{ab} value, though it cannot be applied to such large systems. HDFT would be regarded as a practical alternative to UCCSD(T) even in this d−π conjugated system like the π−π conjugated one.[2,17] The difference between the magnitude of J_{ab}(AP-X) and J_{ab}(X) is not so large in all the models and methods, since the radical orbitals of **1** and **2** exhibit small orbital overlaps, as expected for the magnetic materials.[17−19] Since the difference with respect to J_{ab} values is small in model **a**−**c**, substitution of the phenyl ring with H and CF_3 with CH_3 is not so serious. The magnitude of the J_{ab} values for model **1d** and **1e** is too large as compared with the experimental results.[18,19] These results indicate the necessity of ligands in order to investigate the magnetic interaction quantitatively.

The Mulliken population analysis[45] is often useful for qualitative discussions of charge densities even in d−p systems.[14−16,34] Table 3 shows the population of charge densities obtained on the metal ion M(II), 4-pyridylcarbene group (4-PC), and ligand parts (hfac and acac) for the LS state of models **a**−**e**. The formal charge (2.0) of the divalent manganese ion

(39) Frisch, M. J.; Trucks, G. W.; Schlegel, H. B.; Gill, P. M. W.; Johnson, B. G.; Robb, M. A.;Cheeseman, J. R.; Keith, T. A.; Petersson, G. A.; Montgomery, J. A.; Raghavachari, K.; Al-Laham, M. A.; Zakrzewski, V. G.; Oritiz, J. V.; Foresman, J. B.; Cioslowski, J.; Stefanov, B. B.; Nanayakkara, A.; Challacombe, M.; Peng, C. Y.; Ayala, P. Y.; Chen, W.; Wong, M. W.; Andres, J. L.; Replogle, E. S.; Gomperts, R.; Martin, R. L.; Fox, D. J.; Binkley, J. S.; Defrees, D. J.; Baker, J.; Stewart, J. P.; Head-Gordon, M.; Gonzalez, C.; Pople, J. A. Gaussian, Inc., Pittsburgh, PA, 1995.
(40) Schmidt, M. W.; Baldridge, K. K.; Boatz, J. A.; Elbert, S. T.; Gordon, M. S.; Jensen, J. J.;Koseki, S.; Matsunaga, N.; Nguyen, K. A.; Su, S.; Windus, T. L.; Dupuis, M.; Montgomery, J. A. *J. Comput. Chem.* **1993**, *14*, 1347−1363.
(41) Becke, A. D. *Phys. Rev. A* **l988**, *38*, 3098.
(42) Vosko, S. H.; Wilk L.; Nusair, M. *Can. J. Phys.* **1980**, *58*, 1200.
(43) Lee, C.; Yang, W.; Parr, R. G. *Phys. Rev. B* **l988**, *37*, 785.
(44) Becke, A. D. *J. Chem. Phys.* **l993**, *98*, 5648.
(45) Pople, J. A.; Gill, P. M. W.; Johnson, B. G. *Chem. Phys. Lett.* **l992**, *199*, 557.

Table 3. Charge Densities Calculated for the Lowest-Spin State of Mn(II)(hfac)$_2${di(4-pyridyl)phenylcarbene} (**lz**) and Cu(II)(hfac)$_2${di(4-pyridyl)phenylcarbene} (**2z**) (**z** = **a**−**e**) by the UHF and UB3LYP Methods

		a			b			c			d		e	
M	method	M	4-PC[a]	hfac[b]	M	4-PC[a]	hfac[b]	M	4-PC[a]	acac[c]	M	4-PC[a]	M	4-PC[a]
Mn(II)(**lz**)	UHF	1.703	0.005	−0.856	1.703	0.004	−0.856	1.692	0.008	−0.837	1.653	0.174	1.660	0.170
	UB3LYP	1.258	0.076	−0.704	1.259	0.073	−0.702	1.244	0.055	−0.676	1.083	0.459	1.267	0.367
Cu(II)(**2z**)	UHF	1.583	0.073	−0.861	1.584	0.072	−0.860	1.584	0.052	−0.841	[d]	[d]	1.441	0.280
	UB3LYP	1.003	0.195	−0.656	1.004	0.190	−0.691	0.998	0.160	−0.657	[d]	[d]	[d]	[d]

[a] 4-PC = 4-pyridylcarbene. [b] hfac = hexafluoroacetylacetone. [c] acac = acetylacetone. [d] The calculations were not converged.

Table 4. Spin Densities Calculated for the Lowest-Spin State of Mn(II)(hfac)$_2${di(4-pyridyl)phenylcarbene} (**lz**) (**z** = **a**−**e**) by the UHF and UB3LYP Methods

methods	models	Mn 1[a]	N2[a]	C3[a]	C4[a]	C5[a]	C6[a]	C7[a]	C8[a]
UHF	**1a**	4.945	−0.594	0.632	−0.726	0.829	−0.745	0.643	−2.074
	1b	4.945	−0.603	0.642	−0.739	0.850	−0.759	0.650	−2.137
	1c	4.942	−0.615	0.649	−0.742	0.856	−0.762	0.658	−2.139
	1d	5.094	−0.485	0.465	−0.582	0.673	−0.608	0.479	−2.008
	1e	5.093	−0.505	0.492	−0.616	0.722	−0.641	0.504	−2.100
UB3LYP	**1a**	4.775	−0.128	0.086	−0.179	0.171	−0.198	0.087	−1.620
	1b	4.774	−0.141	0.098	−0.201	0.210	−0.225	0.097	−1.839
	1c	4.767	−0.144	0.098	−0.200	0.211	−0.223	0.097	−1.840
	1d	4.628	−0.130	0.005	−0.010	0.058	−0.114	0.006	−1.389
	1e	4.893	−0.142	0.029	−0.132	0.134	−0.155	0.028	−1.738

[a] These site numbers are shown in **I** of Figure 2.

Table 5. Spin Densities Calculated for the Highest-Spin State of Cu(II)(hfac)$_2${di(4-pyridyl)phenylcarbene} (**2z**) (**z** = **a**−**e**) by the UHF and UB3LYP Methods

methods	models	Cu1[a]	N2[a]	C3[a]	C4[a]	C5[a]	C6[a]	C7[a]	C8[a]
UHF	**2a**	0.872	0.648	−0.619	0.757	−0.843	0.728	−0.643	2.071
	2b	0.872	0.654	−0.624	0.761	−0.844	0.736	−0.649	2.100
	2c	0.874	0.674	−0.641	0.772	−0.857	0.746	−0.666	2.102
	2e	0.957	0.446	−0.439	0.608	−0.679	0.590	−0.467	2.051
UB3LYP	**2a**	0.654	0.271	−0.092	0.239	−0.186	0.204	−0.100	1.609
	2b	0.654	0.274	−0.097	0.251	−0.213	0.216	−0.108	1.792
	2c	0.645	0.269	−0.098	0.251	−0.216	0.214	−0.109	1.794

[a] These site numbers are shown in **I** of Figure 2.

largely decreases because of the increase of CTs from hfac and acac to M(II). The charge density of Cu(II) is smaller than that of Mn(II), indicating that the CT of **2** is larger than that of **1**. The CT increases in the following order: UHF < UB2LYP < UB3LYP < UBLYP. (Table S5) The same tendency is recognized for the CT from the 4-PC group to M(II), in accordance with the trend in the magnitude of the calculated J_{ab} values. In comparison to the charge densities for **a**−**c**, those for **d** and **e** are overestimated, in conformity with the overestimation of the J_{ab} values. The charge distributions are therefore consistent with the conclusion that reasonable computation of J_{ab} values for **a**−**c** by using the UB3LYP method should be due to the decrease of the electron affinity of M(II) to which $(hfac)_2$ is added, and the SE mechanism is operative to determine the sign of them.

The DFT methods usually provide reasonable spin densities for radical species.[46] Table 4 summarizes the population of spin densities for the 4-pyridyl group part of **1a**−**1e**, together with those on Mn(II) and C of the carbene group. Table 5 lists those of **2a**−**2c** and **2e**. Their signs for the 4-pyridyl group change alternately to show the characteristic of the spin density wave (SDW). Both the spin densities of Cu1 and N2 for **2** are positive because of the orthgonality between dσ and pπ orbitals. These results correspond to SP effects.[2,17−19] Judging from the magnitude of the spin density, the UHF overestimates the SP effects of the 4-pyridyl ring. On the other hand, the hybrid methods, especially UB3LYP, estimate the SP effects of the 4-pyridyl ring by spins on the M(II) and carbene sites appropriately. Therefore, it is clear that the hybrid methods are appropriate to elucidate the J_{ab} values for the large d−π−p conjugated systems such as **1a** and **2a**. The difference with respect to the population of spin density is not so large among **a**−**c**.

The ab initio calculations concluded that both the SE and SP effects favor the LS and HS ground states of **1** and **2**, respectively, in accordance with the selection rule in Table 1. This implies that SE- or SP-type explanations of the experiments are feasible for qualitative purposes.[10−12,20]

Natural Orbitals and Orbital Interactions. NOs are visualized for pictorial understanding of the SD and SP effects. The NOs for **1a** by UB3LYP are depicted in Figure 4, and Figure 5 shows the NOs for the HS state of **2a** by UB3LYP. The occupation numbers of HOMO, SOMO, and LUMO for LS states of **1a**−**1e** and those for HS and LS states of **2a**−**2c** and **2e** by UHF, DFT, and their hybrid calculations are summarized in Table 6 and Table 7, respectively.

From Figure 4, the NOs of SOMO+4 and SOMO-4 show the dπ−pπ interaction of the d orbital of the Mn(II) ion and the π orbital of the 4-pyridyl ring, indicating that the Mn(II) ion and carbene show π-type antiferromagnetic SD or SE

(46) Yamanaka, S.; Kawakami, T.; Yamada, S.; Nagao, H.; Nakano, M. Yamaguchi, K. *Chem. Phys. Lett.* **l995**, *240*, 268.

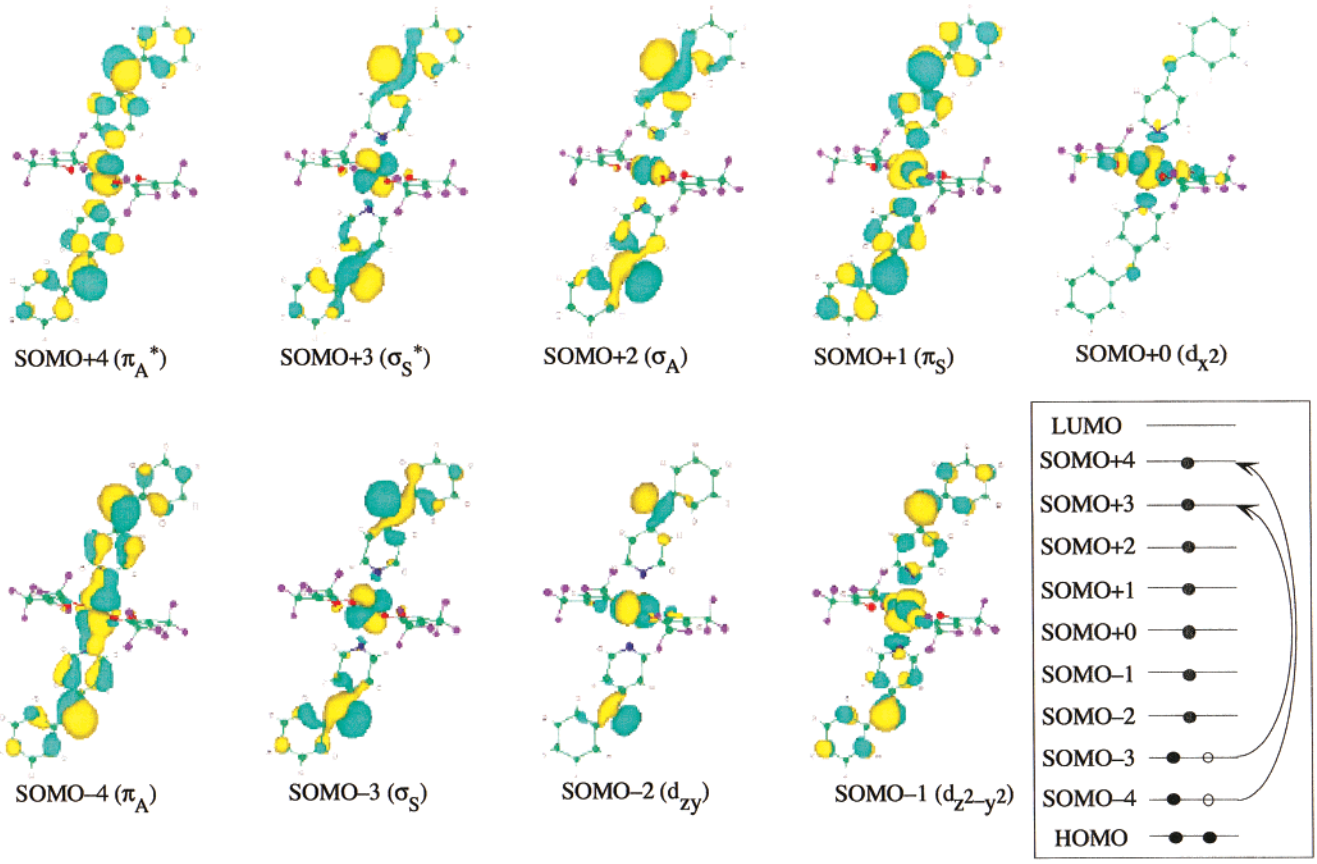

Figure 4. Natural orbitals for the lowest-spin state of **1a** by the UB3LYP calculation.

interaction via the 4-pyridyl ring. The shapes of the three π-NOs (SOMO-4, SOMO+1, SOMO+4) are indeed explained by the pπ−dπ−pπ orbital interactions of the dπ orbital of Mn(II) and pπ orbitals of bis(carbene) as illustrated in **V** in Figure 6. The orbital interaction scheme should be similar even in the case of cis and trans 1:1 Mn(II)(hfac)$_2${(4-pyridyl)carbene} oligomer. The SOMO-3, SOMO+2, and SOMO+3 are regarded as the bonding, nonbonding, and antibonding σ-type NOs, and the corresponding T_i value for **1a** by UB3LYP is only 0.004, indicating that the SE interaction via the σ-type interaction is weak.

From Table 6, the T_i values of SOMO ± 4 are 0.04 and 0.10 by UHF and UB3LYP, respectively, indicating that the π-type SOMO−SOMO interaction by UHF is weak. We found that UHF underestimates the SD (or SE) interactions. The small (large) magnitude of the J_{ab} value by UHF is due to a small SE effect, while UB3LYP can deal with it appropriately because of 80% mixing of the BLYP component.[44] The occupation numbers of HOMO and LUMO are 1.862 and 0.138 by UHF, respectively. This indicates the strong SP effect of the closed-shell orbitals under the UHF approximation as illustrated by **IIIc** in Figure 2. Judging from the occupation numbers, the SP effect is rather weak by UB3LYP. The occupation numbers of the three d orbitals are 1.0, showing no significant contribution to the SE interaction. The NO analysis clearly demonstrates that the origin of the antiferromagnetic exchange interaction for **1a** is the pπ−dπ−pπ SE interaction as illustrated by **IVa** and **IVb** in Figure 4 and **V** in Figure 6, together with the SP of the π network.[17−19]

The five NOs in Figure 5 are singly occupied since $S_{max} = {}^5/_2$. The π-type SOMO+2 and SOMO-2 are mainly localized on the right and left pyridylcarbene groups, respectively. The σ-type SOMO+1 and SOMO-1 also show the same tendency, while the nonbonding σ-NO (SOMO+0) is mainly localized on the central Cu(II) plus (hfac)$_2$ group. Considering the orthogonality between the σ and π orbitals in each 4-PC group, the parallel spin alignment is preferable at the carbene site. The ferromagnetic SE interaction of the central σ orbital with the π orbitals is also expected since the σ center has the small tails on the carbene sites and the π orbital (SOMO-2) has the small tail on the central Cu(II) ion. The NO analysis clearly indicates an important role for one-center exchange interaction suggested by Musin and Morokuma.[20] Figure 6 illustrates these ferromagnetic SE interactions **VI** and **VII** at the Cu(II) and carbene sites, respectively.

As summarized in Table 7, the T_i values of SOMO ± 2 at the LS state of **2a** show that the σ-type antiferromagnetic SE interaction between the Cu(II) ion and triplet carbenes via the 4-pyridine ring is rather weak. On the other hand, the π-type SE interaction is negligible, as can be recognized from the fact that their occupation numbers are 1.0. This situation is quite different from that of **1a**. The occupation numbers of HOMO and LUMO for **2a** by UHF also show the large and small contributions of the SP effect, respectively. The J_{ab} values of **2a** become ferromagnetic since the ferromagnetic Coulombic and SE interactions outweigh the antiferromagnetic σ-type SE interaction, and the ferromagnetic SP effect is also operative.

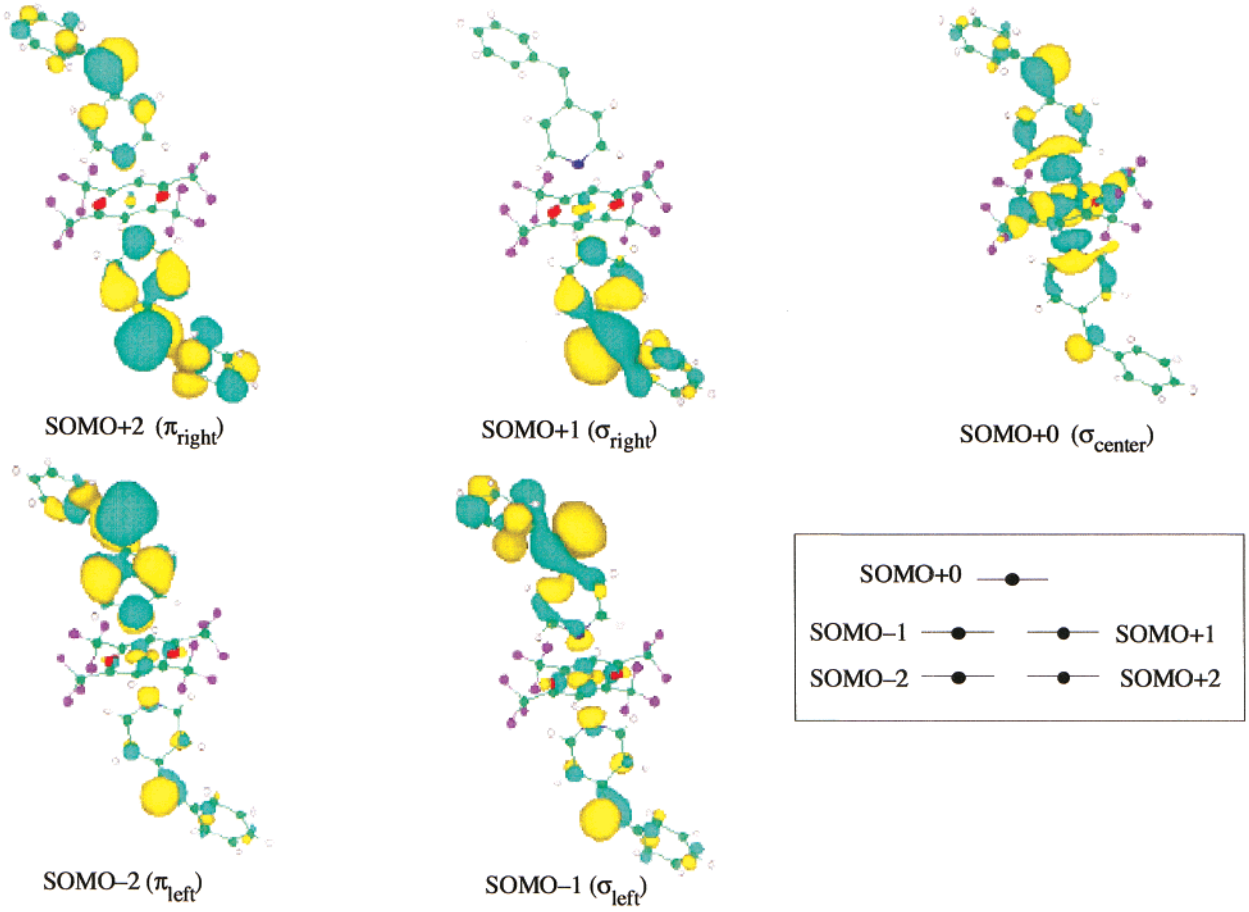

Figure 5. Natural orbitals for the highest-spin state of **2a** by the UB3LYP calculation.

Table 6. Occupation Numbers of the Natural Orbitals for the Lowest-Spin State of Mn(II)(hfac)$_2${di(4-pyridyl)phenylcarbene} (**lz**) (**z** = **a**−**e**) by the UHF and UB3LYP Methods

methods	models	HOMO	SOMO-4	SOMO-3	SOMO-2 to +2	SOMO+3	SOMO+4	LUMO
UHF	**1a**	1.862	1.038	1.001	1.000	0.999	0.962	0.138
	1b	1.867	1.040	1.002	1.000	0.998	0.960	0.133
	1c	1.866	1.039	1.002	1.000	0.998	0.961	0.134
	1d	1.876	1.051	1.003	1.000	0.997	0.949	0.124
	1e	1.906	1.049	1.003	1.000	0.997	0.951	0.094
UB3LYP	**1a**	1.993	1.103	1.004	1.000	0.996	0.897	0.007
	1b	1.992	1.103	1.009	1.000	0.991	0.897	0.008
	1c	1.992	1.109	1.011	1.000	0.989	0.981	0.008
	1d	1.994	1.671	1.018	1.000	0.982	0.329	0.006
	1e	1.993	1.390	1.021	1.000	0.979	0.610	0.007

Table 7. Occupation Numbers of the Natural Orbitals for the Highest- (HS) and Lowest-Spin (LS) State of Cu(II)(hfac)$_2${di(4-pyridyl)phenylcarbene} (**2z**) (**z** = **a**−**e**) by the UHF and UB3LYP Methods

		HS			LS				
methods	models	HOMO	SOMO-2 to +2	LUMO	HOMO	SOMO-2	SOMO-1 to +1	SOMO+2	LUMO
UHF	**2a**	1.866	1.000	0.134	1.869	1.001	1.000	0.999	0.131
	2b	1.868	1.000	0.132	1.872	1.002	1.000	0.998	0.128
	2c	1.863	1.000	0.137	1.867	1.002	1.000	0.998	0.133
	2e	1.916	1.000	0.084	1.918	1.011	1.000	0.989	0.082
UB3LYP	**2a**	1.992	1.000	0.008	1.993	1.013	1.000	0.987	0.007
	2b	1.990	1.000	0.010	1.992	1.021	1.000	0.980	0.008
	2c	1.990	1.000	0.010	1.992	1.021	1.000	0.979	0.008

The ab initio calculations are consistent with the SP plus SD rules for **2a** in Table 1.

However, the exact calculation of relative contributions of the SD and SP effects remains a difficult task because they are sensitive to quality of basis sets and extent of correlation corrections. For example, UNO analysis of **1a** and **2a** indicate that UNO CASCI {9, 9} and {5, 5} are necessary for discussion of the SOMO−SOMO interactions, while UNO CASCI {25,

Table 8. Effective Exchange Integrals (J_{ab})[a] Calculated for Mn(II)(4-pyridyl)carbene (**Ia**), Cu(II)(4-pyridyl)carbene (**Ib**), and Mn(II)(3-pyridyl)carbene (**Ic**) by the UHF, UMP2(4), UCCSD(T), HDFT, and CASCI Methods

	Ia[b]		**Ib**[c]		**Ic**	
methods X	J_{ab}(X)	J_{ab}(AP-X)	J_{ab}(X)	J_{ab}(AP-X)	J_{ab}(X)	J_{ab}(AP-X)
broken symmetry						
UHF	−65.42	−65.70	184.4	181.6	58.54	58.23
UMP2	−8.377	−8.401	202.1	200.0	−15.77	−15.71
UMP4	−22.24	−22.31	320.8	317.4	−6.762	−6.734
UCCSD(T)	−56.50	−56.67	229.2	231.6	3.110	3.097
UB3LYP	−288.9	−281.2			−174.3	−169.5
symmetry-adapted						
UNO CASCI {SOMO−SOMO}[d]		−34.36		33.80		−0.197
UNO CASCI {m, m}[e]		−26.99		48.87		3.862

[a] J_{ab} are shown in cm^{-1}. [b] J_{ab} from experiment is $-12.37\ cm^{-1}$. [c] J_{ab} from experiment is $46.43\ cm^{-1}$. [d] SOMO = 7 for **Ia** and **Ic**, and SOMO = 3 for **Ib**. [e] $m = 11$ for **Ia** and **Ic**, and $m = 9$ for **Ib**.

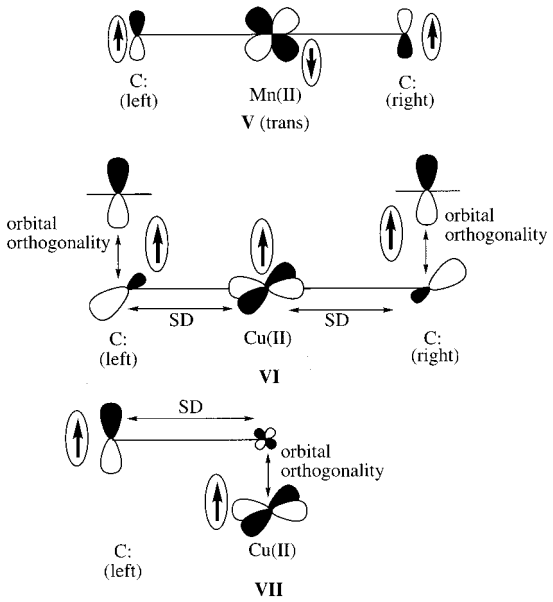

Figure 6. Orbital interaction schemes for π-type antiferromagnetic superexchange interaction **V** of {**1a** (**3T**) and **3C**}, and $\sigma-\sigma$-type ferromagnetic superexchange interactions (**VI** and **VII**) for **2a**.

25} and {21, 21} are inevitable for evaluation of SP and other effects because CAS {18, 18} is responsible for through-bond interactions via the π network. Since such large CI calculations are impossible, computaions of model systems are inevitable.

Comparisons with the Post HF Results of the Simplest Models Ia, Ib, and Ic

As mentioned above, it is desirable to perform post HF calculations as well as UHF and HDFT in order to elucidate the magnetic interaction for d−π−p conjugated systems. Table 8 summarizes the calculated J_{ab} values for **Ia** and **Ib**, together with those of Mn(II)3-pyridylcarbene (**Ic**). All the calculated J_{ab} values for **Ia** are negative, reproducing the antiferromagnetic interaction determined by the experiment qualitatively.[10] The magnitude by the UCCSD(T) value is too large as compared to the experimental value ($-12.37\ cm^{-1}$). This trend becomes more remarkable in the case of BLYP and B3LYP, while all the calculated J_{ab} values for **Ib** show the ferromagnetic interaction determined by the experiments.[11,12] But the magnitude by the UMP2(4) value is too large as compared to the experimental value ($46.43\ cm^{-1}$). Coordination of ligands such as hfac and acac to M(II) ions removes such overshooting, because $(hfac)_2$ and $(acac)_2$ decrease the electron affinity of M(II) ions, in other words, the charge transfer from 4-PC to M(II) ions. The calculated results in Tables 2 and 8 show that the coordination ligands are crucial in order to estimate the magnetic interaction for these d−π−p conjugated systems. The UCCSD(T) or QCISD computations of **a**−**c** should provide the same conclusion, though those are impossible in our computer system.

Both the UNO CASCI {7, 7} for **Ia** and {3, 3} for **Ib** would provide the SOMO−SOMO interaction. On the other hand, UNO CASCI {11, 11} and {9, 9} include both the SP and higher-order correlation correction (EC) terms.[32] The J_{ab} values via the SOMO−SOMO interactions of **Ia** and **Ib** are −34.36 and 33.80 cm^{-1}, while, the UNO CASCI {11, 11} for **Ia** and {9, 9} for **Ib** are −26.99 and 48.87 cm^{-1}, respectively. Using the J_{ab} values by CASCI calculations, we can estimate the SP and EC effects by the π orbital in the pyridine ring. These effects are 7.37 cm^{-1} for **Ia** and 15.07 cm^{-1} for **Ib**, respectively, and smaller than SOMO−SOMO interactions, also showing that the SP effect is less effective for the magnetic interaction of **Ia** and **Ib**.

The J_{ab} values for **Ic** by UHF and UCCSD(T) are positive, in accordance with the topological rule,[2,6,17−19,47−49] based on the SP effect, but they are negative under the UMP2(4) approximation. The tendency is similar to that of *m*-phenylene-bridged polyradicals.[2] The UB3LYP also predicts the large negative J_{ab} values because of the large estimation of the SE interaction. The large estimation by HDFT is responsible for the loss of ligand coordination. The magnitude of the calculated J_{ab} values would be largely decreased by the coordination of ligands to Mn(II). The J_{ab} value by UNO CASCI {7, 7} for **Ic** indicates small antiferromagnetic interaction between SOMOs because of the SE interactions, while that by UNO CASCI {11, 11} shows small ferromagnetic interaction because of the inclusion of SP and EC interactions. The CASCI computations clearly demonstrate that SD and (SP + EC) effects are competitive for *m*-phenylene-bridged d−p complexes, supporting the selection rule in Table 1. The sign of J_{ab} should be dependent on ligands and conformational effects of the phenyl group as well as radical groups in these systems. In fact, the experimental results by the Koga and Iwamura group[10−12,49] showed that the J_{ab} values of the meta analogues of **1**, **2**, and **3** are essentially zero because of this competition. On the other

(47) (a) Yamaguchi, K.; Toyoda, Y.; Fueno, T. *Synth. Met.* **1987**, *19*, 81. (b) Yamaguchi, K.; Toyoda, Y.; Nakano, M.; Fueno, T. *Synth. Met.* **1987**, *19*, 87.
(48) Takui, T.; Kita, S.; Ichikawa, S.; Teki, Y.; Kinoshita, T.; Itoh, K. *Mol. Cryst. Liq. Cryst.* **1989**, *176*, 67.
(49) Iwamura, H. *Pure Appl. Chem.* **1993**, *65*, 57.

hand, the SP effect is predominant for Cr(III) complex with *m*-phenylene radical as discussed below.

Discussion

Difference in the Magnetic Interaction between Mn(II) and Cu(II) Ions. We discuss the difference in the J_{ab} values between Mn(II) and Cu(II) ions using the intermolecular CI model and the above results. Since the Mn(II) ion in **1** contains five unpaired d electrons, Mn(II) complex **1** shows dπ−pπ, dσ−pσ, and dσ−pπ interactions. NO analysis of **1a** and CASCI calculation for the simplest model **Ia** show that dπ−pπ interaction is more effective to the magnetic interaction than other interactions. Judging from the intermolecular CI model, Mn(II)−carbene complex **1a** shows an antiferromagnetic coupling because the dπ−pπ interaction gives rise to an antiferromagnetic interaction. On the other hand, Cu(II) ion in **2** contains one unpaired d electron which occupied the $d_{x^2-y^2}$ orbital. NOs and their occupation numbers of **2a** and CASCI calculation of **Ib** indicate the d unpaired electron contributes to dσ−pσ and dσ−pπ. According to the CI model, the dσ−pσ and dσ−pπ couplings for **2a** provide a ferromagnetic interaction.

In conclusion, the difference in the symmetries[32] of the magnetic orbitals occupied by d unpaired electrons between Mn(II) and Cu(II) gives rise to the difference of orbital interaction, dπ−pπ interaction, or dσ−pσ and dσ−pπ interaction, leading to the antiferromagnetic interaction of **1** and ferromagnetic interaction of **2**.

Dependence of the Model on the Magnetic Interaction for 1 and 2. Here, we consider the dependence of the model on the J_{ab} values and charge and spin density distributions in order to understand what controls the magnetic interaction. The J_{ab} value and charge and spin density distributions for **a**−**c** are similar, indicating that the change of groups from hfac to acac or from phenyl group to H is hardly effective to these properties. No hfac or acac ligand model cannot provide the appropriate charge or spin density distributions. **1b**, **1c**, and **2c** obtained by addition of acac ligand to **1d**, **1e,** and **2e** show the proper J_{ab} values and charge and spin density distributions. Compared with **Ia** and **1e**, the J_{ab} values are reduced from −281.2 to −73.76 cm^{-1} by the UB3LYP method. We find that the coordination effect of 4-PC to Mn(II) ion plays a key role in the J_{ab} values for **1**. NOs in Figure 5 also show that the coordination effect of 4-PC is important for the J_{ab} value. In addition, the J_{ab} value is close to the experimental result, when the ligand such as hfac and acac are coordinated to Mn(II).

Then it is concluded that the ligand coordination effects of both 4-pyridylcarbene and hfac or acac play a crucial role for the determination the J_{ab} values, but the ligand coordination effect of hfac or acac is more important for the active control of charge and spin density distributions.

Spin Alignment Rules in d−π−p Conjugated Polyradicals. Recently, several transition metal−radical complexes have been synthesized, and their magnetic properties have been elucidated experimentally.[1,6,10−12] Figure 7 illustrates the molecular structures of such species (**1Z**−**12Z**), which are classified into *p*-phenylene and *m*-phenylene types, depending on the positions of radical groups: phenyl carbene group (**A**) and *tert*-butyl nitroxide (**B**). Table 1 summarizes the observed J_{ab} values for **1Z**−**12Z**. It is seen from Table 1 and the present theoretical results that both the SE and SP effects favor the LS ground state of 1:2 Mn(II)(hfac)$_2$(*p*-phenylene-type radical)$_2$ complexes and 1:1 Mn(II)(hfac)$_2$(*p*-phenylene-type radical) polymers (oligomers), predicting the total negative (antiferromagnetic) J_{ab} values. The experimental results[6,10−12] are completely compatible with the SP plus SD rules[2,17−19,21,47] for molecular magnets. On the other hand, the sign of the total J_{ab} values is determined by subtle balances between the SD ($J < 0$) and SP ($J > 0$) effects in the cases of 1:2 Mn(II)(hfac)$_2$(*m*-phenylene-type radical)$_2$ complexes and 1:1 Mn(II)(hfac)$_2$(*m*-phenylene-type radical) polymers (oligomers). The experimental χT plots for these species[10−12] indicated that the J_{ab} values are essentially zero.

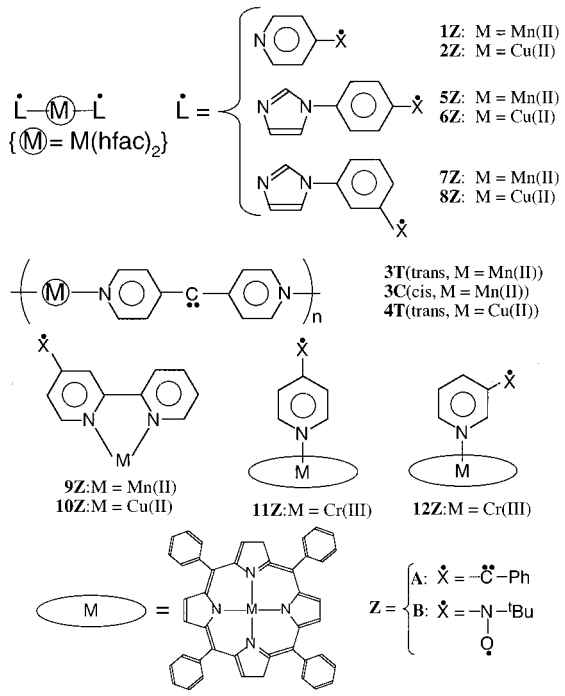

Figure 7. The d−p conjugated magnetic systems (**1**−**12**) with *p*- or *m*-phenylene-type bridges. M means transition metals such as Mn(II) and Cu(II). The observed J_{ab} values for these species are given in Table 1.

Both the SD and SP effects predict the ferromagnetic exchange interactions in the cases of 1:2 Cu(II)(hfac)$_2$(*p*-phenylene-type radical)$_2$ complexes and 1:1 Cu(II)(hfac)$_2$(*p*-phenylene-type radical) polymers (oligomers). The available experimental results are consistent with the SP plus SD rule as shown in Table 1. On the other hand, the SD and SP effects are competitive in the cases of the corresponding *m*-phenylene-type radical complexes such as **8B**. The experiments for **8B** demonstrated the total antiferromagnetic interaction, leading to the conclusion that the SP effect overweighs the SD effect in the Cu(II) complexes with a *m*-phenylene bridge.

The SP plus SD rules in Table 1 are consistent for the experimental results for tetraphenylporphyrine (TPP)−chromium(III) complexes with *p*- or *m*-phenylene-type radical (**11B**, **12B**). The observed J_{ab} value for the para isomer (**11B**) was antiferromagnetic because of dπ−pπ interaction as **1**, while it became ferromagnetic for the meta isomer (**12B**).

Design of magnetic polymers and dendrimers[1,8,49] is also feasible on theoretical and experimental grounds as summarized in Table 1. In fact, many applications of these rules to d−p conjugated polyradicals are conceivable. Synthesis of such novel systems is interesting not only for photoinduced magnetism but

also for magnetooptics[50] and optoelectronics.[51] Bose−Einstein condensation of singlet or triplet exciton[52] will be an interesting future problem in these dendrimers.[53]

Application of the **Approximate Spin Projection Method for BS DFT Solution.** Our AP scheme[2,17,27,54] is applicable to BS solutions, for which the orbital overlaps (T_i) between magnetic orbitals are not negligible. The total energy of the LS state is given by the AP scheme[2,17] as

$$^{\mathrm{AP-LS}}E_{\mathrm{X}} = {}^{\mathrm{LS}}E_{\mathrm{X}} + J_{\mathrm{ab}}(\mathrm{AP-X})[{}^{\mathrm{LS}}\langle S^2\rangle - S_{\mathrm{min}}(S_{\mathrm{min}}+1)] \quad (8)$$

where S_{min} is the spin angular momentum of the LS state. This equation removes the major part of the spin contamination errors, being applicable to depiction of potential curves as shown previously.[17,55] In fact, eq 8 works well in the whole region of dissociation processes of covalent bonds since the AP-LS energy reduces to LS energy of the closed-shell state at the instability threshold $T_i = 1$.[27]

The AP scheme in eq 8 is applicable to full or partial geometry optimizations of the Mn(II) complexes **1z** (**z** = **a**−**c**) and Cu(II) complexes **2z** (**z** = **a**−**c**), though we have not performed such expensive computations. From the experimental J_{ab} values for **1a**, **3T**, and **3C** presented in Table 1, it is clear that their magnitude is sensitive to geometries and solid-state structures, though the sign is not changed. Therefore, the geometry optimizations of **1z** (**z** = **a**−**c**) and **2z** (**z** = **a**−**c**) are interesting future problems for quantitative calculations of J_{ab} values. Applications of the AP scheme to radical reactions[55] have attracted recent interest in relation to biologically important binuclear transition metal complexes involved in enzymes.[55,56] Since the J_{ab} values for these complexes have been determined experimentally, the AP-DFT calculations of them are effective for examination of the reliabilities of the DFT solutions (UBLYP, UB3LYP, and others) for searching transition structures of enzyme reactions. In fact, they are successfully applied to depict potential curves for addition and dissociation reactions between hemocyanin and molecular oxygen.[55]

Concluding Remarks

UHF and HF plus DFT hybrid calculations were performed for **1a**, **2a**, and their models to elucidate the mechanisms of effective exchange interactions between transition metal ion and carbene sites. The NO analyses of these solutions followed by UNO CASCI are very useful for the purpose. Our conclusions are as follows: (i) Mn(II) complex **1a** shows an antiferromagnetic interaction because of the π-type antiferromagnetic SE effect and the π-type SP effect; (ii) the positive J_{ab} value for Cu(II) complex **2a** is explained by the fact that ferromagnetic SE interactions due to orbital orthogonality and the σ-type ferromagnetic SP effect are more effective than the σ-type antiferromagnetic SE interaction; (iii) both the ligand coordination effects play a crucial role in the J_{ab} value; (iv) the ligand coordination effect of hfac is important to the appropriate charge or spin densities; (v) the UB3LYP calculation provides reasonable effective exchange integrals for **1a** and **2a**; (vi) the SP plus SD (SE) rules in Table 1 are reliable on theoretical grounds, together with the experiments available; (vii) the interplay between theory and experiment leads to molecular design of possible d−π conjugated magnetic polymers and dendrimers.

Acknowledgment. This work has been supported by Grants-in-Aid for Scientific Research on Priority Areas (11119240 and 10149105) from the Ministry of Education, Science, Sports and Culture, Japan. K.Y. thanks Professor J. Furukawa for his encouragement and discussions. We thank Professor Keiji Morokuma for helpful discussions. Y.T. is also supported by Research Fellowships of the Japan Society for the Promotion of Science for Young Scientists.

Supporting Information Available: The total energies and total angular momentums for **1z** (Table S1), **2z** (**z** = **a**−**e**) (Table S2), **Ia**, **Ib,** and **Ic** (Table S3 and S4). The charge and spin densities for **1z** and **2z** (Table S5−S7) by UHF, spin-polarized Becke half and half LYP (UB2LYP), UB3LYP, and UBLYP. The more detailed occupation numbers of **1a**−**1e** and **2a**−**2e** (Table S8−S10) calculated by UHF, spin-polarized Becke half and half LYP (UB2LYP), UB3LYP, and UBLYP calculations and the occupation number from HOMO+8 to LUMO-8 of UNO of **1a** and **2a** (Table S11). The color graphics of the natural orbitals of **1b** and **1c** (Figure S1 and S2) in LS state and **2a** in LS state and **2b** and **2c** (Figure S3−S7) in both HS and LS state by UB3LYP calculations (PDF). This material is available free of charge via the Internet at http://pubs.acs.org.

JA015967X

(50) Kiribayashi, S.; Kobayashi, T.; Nakano, M.; Yamaguchi, K., *Int. J. Quantum Chem.* **l999**, *75*, 637.
(51) (a) Yamaguchi, K. In *Electronic and Optical Functional Polymers*; Yoshino, K., Ed.; Koudansha Scientific: Tokyo, 1990; Chapter 12 (in Japanese). (b) Nakano, M.; Fujita, H.; Takahata, M.; Yamaguchi, K. *J. Chem. Phys.* **2001**, *115*, 1052.
(52) Kotori, H.; Ido, T.; Isoda, Y.; Kuwata-Gonokami, M. *Phys. Rev. Lett.* **l999**, *82*, 1116.
(53) Nagao, H.; Nakano, M.; Ohta, K.; Shigeta, Y.; Kiribayashi, S.; Yoshioka, Y.; Yamaguchi, K. *Mol. Cryst. Liq. Cryst.* **2000**, *342*, 273.
(54) (a) Yamaguchi, K.; Jensen, F.; Dorigo, A.; Houk, K. N. *Chem. Phys. Lett.* **l988**, *149*, 537. (b) Yamaguchi, K.; Takahara, Y.; Fueno, T.; Houk, K. N. *Theor. Chim. Acta* **l988**, *73*, 337. (c) Isobe, H.; Takano, Y.; Kitagawa, Y.; Kawakami, T.; Yamanaka, S.; Yamaguchi, K.; Houk, K. N. *Mol. Phys*., in press.
(55) (a) Yoshioka, Y.; Kubo, S.; Yamaguchi, K.; Saito, I. *Chem. Phys. Lett.* **l998**, *294*, 459. (b) Takano, Y.; Kubo, S.; Onishi, T.; Isobe, H.; Yoshioka, Y.; Yamaguchi, K. *Chem. Phys. Lett.* **2001**, *335*, 395.
(56) (a) Siegbahn, P. E. M.; Blomberg, M. R. A. *Annu. Rev. Phys. Chem.* **1999**, *50*, 221. (b) Siegbahn, P. E. M.; Blomberg, M. R. A. *Chem. Rev.* **2000**, *100*, 421.